Small-Angle Neutron Scattering Studies on Chain Asymmetry of Coextruded Poly(vinyl alcohol) Film

Mitsuhiro Shibayama,* Hidenobu Kurokawa, and Shunji Nomura

Kyoto Institute of Technology, Matsugasaki, Kyoto 606, Japan

Saroj Roy† and Richard S. Stein

Polymer Research Institute, University of Massachusetts, Amherst, Massachusetts 01003

Wen-li Wu*

National Institute of Standards and Technology, Gaithersburg, Maryland 20899.
Received April 18, 1989; Revised Manuscript Received September 1, 1989

ABSTRACT: Chain asymmetry of solid-state coextruded poly(vinyl alcohol) film (PVA) was studied by using small-angle neutron scattering. The radius of gyration, R_g, was estimated by a nonlinear least-square regression analysis with a theoretical scattered intensity function that is based on a model of deformed Gaussian chains. The R_g for undeformed chains was estimated to be $R_g = 2.43\langle n\rangle_z^{1/2}$ Å, where $\langle n\rangle_z$ is the z-average degree of polymerization of PVA. The R_g values for deformed PVA indicate that the poly(vinyl alcohol) chains are deformed affinely at least up to the extension draw ratio of ca. 5, which is in good accordance with the results of birefringence measurement.

Introduction

Studies of chain asymmetry of deformed polymer systems are of importance from both the industrial and academic points of view. Recent developments of small-angle neutron scattering provide a direct evaluation of chain asymmetry. Hadziioannou et al.[1] reported that polystyrene, having a degree of polymerization greater than that required for entanglements, was deformed affinely up to an extension draw ratio of ca. 10. This is the case of amorphous polymers. In the case of crystalline polymers, such as high-density polyethylene, Lo[2] showed that chains are deformed more or less affinely up to an extension draw ratio (EDR) of 5 and then become less deformed than the value expected from affine deformation. They explained this behavior with reorganization and chain slippage.

Poly(vinyl alcohol) (PVA) is a crystalline polymer for which the local conformation in bulk is not well understood. A fringed-micelle type structure has been accepted for a long time for PVA film prepared from aqueous solution. On the other hand, folded-chain crystals are observed if it is solidified from an organic solvent.[3] It is natural to expect that intra- and interchain hydrogen bonds play an important role in local chain organization. On deformation, these hydrogen bonds may work as cross-linking points or entanglements. Since PVA is a polymer widely used in industry,[4] e.g., fibers, staples, asbestos alternatives, sheet, high oxygen barrier film, and so on, it is worthwhile to explore chain asymmetry of deformed PVA fibers and/or films.

In this paper, we examine the radii of gyration of a solid-state coextruded PVA film cast from aqueous solution in both the extension and the perpendicular directions by small-angle neutron scattering and compare the results with those of polystyrene.

Theoretical Background

Theoretical scattered intensity functions for a deformed chain depend greatly on the model of deformation. For example, the affine deformation model, the end-to-end pulling model, and the phantom network model are presented in the literature,[5-8] particularly to describe deformation of polymer networks. We employ here the affine deformation model because of its simplicity and examine how experimental results deviate from the value expected from this model.

The segment distribution function for a pair of segments i and j on a deformed Gaussian chain, $W_{i,j}(\mathbf{r})$, is given by

$$W_{i,j}(\mathbf{r}) = C\exp\{-3\mathbf{r}^t\mathbf{A}^{-1}\mathbf{r}/(2|i-j|b^2)\} \quad (1)$$
$$C = (3/2\pi|i-j|b^2|\mathbf{A}|)^{3/2}$$

where b is the segment length. $\mathbf{A}$ is the strain matrix, $\mathbf{A}^{-1}$ is the inverse matrix of $\mathbf{A}$, and $\mathbf{r}^t$ is the transposed vector of $\mathbf{r}$. In the case of affine deformation $\mathbf{A}$ is given by

$$\mathbf{A} = \begin{bmatrix} \alpha^2 & 0 & 0 \\ 0 & \alpha^{-1} & 0 \\ 0 & 0 & \alpha^{-1} \end{bmatrix} \quad (2)$$

where α is the macroscopic draw ratio in the principal direction. The Fourier transform of $W_{i,j}(\mathbf{r})$ is given by

$$W_{i,j}(\mathbf{q}) = \exp\{-|i-j|b^2\mathbf{q}^t\mathbf{A}\mathbf{q}/6\} \quad (3)$$

where $\mathbf{q}$ is the scattering vector. The single-chain structure factor $P(\mathbf{q})$, i.e., the intrachain scattered intensity function, is obtained by

$$P(\mathbf{q}) = \sum_i^n\sum_j^n W_{i,j}(\mathbf{q})$$
$$= 2\{e^{-u} - 1 + u\}/u^2 \quad (4)$$

where n is the degree of polymerization of the chain and

$$u = nb^2\mathbf{q}^t\mathbf{A}\mathbf{q}/6 \quad (5)$$

The absolute scattered intensity $I(q)$ from a homogeneous mixture of deutereous and hydrogenous polymer

* To whom correspondence should be sent.
† Present address: Polaroid Corporation, 750 Main Street, Cambridge, MA 02139.

chains having equal degrees of polymerization is given by

$$I(\mathbf{q}) = K\phi_d\phi_h nP(\mathbf{q}) \quad (6)$$

where ϕ_i is the volume fraction of the i component. K is the contrast factor given by

$$K = N[(a_d/v_d) - (a_h/v_h)]^2 v_d \quad (7)$$

where N is Avogadro's number and a_i and v_i are the scattering length and monomer volume of the i component. When the degrees of polymerization of d and h chains are different, $I(\mathbf{q})$ is modified in terms of sum rule and is given by[9]

$$KI^{-1}(\mathbf{q}) = [n_d\phi_d P_d(\mathbf{q})]^{-1} + [n_h\phi_h P_h(\mathbf{q})]^{-1} \quad (8)$$

where $P_i(\mathbf{q})$ is the single-chain structure factor of component i. In eq 8 the Flory interaction parameter was assumed to be zero.[10] If the system is a mixture of polydisperse polymers, eqs 5 and 8 are modified as

$$u = \langle n\rangle_z b^2 \mathbf{q}^t\mathbf{A}\mathbf{q}/6 \quad (9)$$

$$KI^{-1}(\mathbf{q}) = [\langle n_d\rangle_w\phi_d P_d(\mathbf{q})]^{-1} + [\langle n_h\rangle_w\phi_h P_h(\mathbf{q})]^{-1} \quad (10)$$

where $\langle n_i\rangle_w$ and $\langle n_i\rangle_z$ are weight- and z-average degrees of polymerization of component i. Although eqs 8 and 10 are derived for an undeformed polymer mixture, the sum rule on reciprocal intensity is valid also for deformed chains.

If the magnitude of $\mathbf{q}$ is small, eq 10 can be expanded as

$$P_i(\mathbf{q}) = 1 - (1/3)(R_{g,i})_0^2\mathbf{q}^t\mathbf{A}\mathbf{q} + \ldots \quad (11)$$

where

$$(R_{g,i})_0 = (\langle n_i\rangle_z b^2/6)^{1/2} \quad (12)$$

is the radius of gyration of undeformed chains of type i. Therefore, the scattered intensity along any direction can be expressed as a function of q, the magnitude of $\mathbf{q}$, and the radius of gyration along the same direction.

$$KI^{-1}(q) = [\langle n_d\rangle_w\phi_d]^{-1} + [\langle n_h\rangle_w\phi_h]^{-1} + [R_{g,d}^2/(3\langle n_d\rangle_w\phi_d) + R_{g,h}^2/(3\langle n_h\rangle_w\phi_h)]q^2 + \ldots \quad (13)$$

Evaluation of R_g values in the extension direction becomes difficult with increasing extension draw ratio (EDR) or the value of α because (1) as the radius of gyration becomes bigger, the Guinier region, $q < 1/R_g$, approaches the instrument limit and (2) the instrumental smearing effects become significant when the system is highly oriented. These problems were discussed by Ullman,[11,12] Wignall et al.,[13] and Tanzer and Crist.[14]

Hadziioannou et al.[1] used the technique of equal intensity contour patterns and its relationship between the molecular draw ratio, MDR, and q values

$$\mathrm{MDR} = (q_\perp/q_\parallel)^{2/3} = (R_{g\parallel}/R_{g\perp})^{2/3} \quad (14)$$

where $R_{g\perp}$ and $R_{g\parallel}$ are the radii of gyration perpendicular and along the extension direction. They evaluated $R_{g\perp}$ from a Zimm plot (eq 13) and estimated $R_{g\parallel}$ using eq 14. This technique, however, does not give a unique R_g value and its value changes depending on the contour (isointensity curve) chosen. This is simply due to the fact that the scattered intensity cannot be expressed by a simple Guinier function, $I \sim \exp(-R_g^2q^2/3)$, over a broad q range.

In principle, these problems make it difficult to estimate a large R_g from an asymmetrical scattering pattern since it is almost impossible to remove the instrumental smearing effect completely. A model or a scattering function has to be chosen a priori for most cases. We chose the Debye function for the theoretical scattered intensity function. The validity of the Debye function for deformed PVA chains is still an open question because PVA is a semicrystalline polymer. However, the Debye function is one of the best approximate functions for scattered intensity from polymer chains if one restricts the q range, e.g., $qR_g \simeq 1$. Tanzer et al.,[15] for example, used the Debye function to describe scattering behavior for melt-crystallized polybutadienes. By fitting an observed scattered intensity with the theoretical function, one can obtain R_g and the weight-average molecular weight. The details of the curve-fitting method are described elsewhere for the case of undeformed chains.[16] This procedure was conducted on the scattered intensity curves both for the extensional and perpendicular directions.

PVAs studied here were polymerized by radical polymerization of vinyl acetate, followed by saponification of poly(vinyl acetate). Therefore PVAs are expected to have a most probable distribution of degree of polymerization. The ratios of the number-, viscosity-, weight-, and z-average degree of polymerization, $\langle n\rangle_n$, $\langle n\rangle_v$, $\langle n\rangle_w$, and $\langle n\rangle_z$, are given by[18]

$$\langle n\rangle_n:\langle n\rangle_v:\langle n\rangle_w:\langle n\rangle_z = 1:1.77:2:3 \quad (15)$$

Table I
Sample Characteristics

code	$\langle n\rangle_v$	% saponification	% deuteration[a]	stereoregularity[b] I	H	S
d-PVA900	900	99.60	50.1	21.6	48.3	30.1
d-PVA1850	1850	99.49	94.41	21.51	49.34	29.14
h-PVA1750	1750	98.50	0.0	21.5	49.6	28.9

[a] Due to the isotope substitution reaction, the percent deuteration is calculated with respect to C_2D_3OH instead of C_2D_4O. [b] Triad tacticities, iso (I), syndio (S), and hetero (H) were measured by 500-MHz ^{1}H NMR.

Experimental Section

1. Samples. Deutereous and hydrogenous poly(vinyl alcohol)s were supplied by Kuraray Co., Ltd. (Certain commercial materials and equipment are identified in this paper in order to specify adequately the experimental procedure. In no case does such identification imply recommendation or endorsement by the National Institute of Standards and Technology, nor does it imply necessarily the best available for the purpose.) The details of the preparation of the deutereous poly(vinyl alcohol) are described elsewhere.[19] Table I shows the sample characteristics of the deutereous and hydrogenous poly(vinyl alcohol)s. They are coded as d-PVA and h-PVA followed by the viscosity-average degree of polymerization, respectively. The viscosity-average degree of polymerization was measured by viscometry by using the following equations[20]

$$[\eta] = 8.29 \times 10^{-4}\langle n\rangle_v^{0.62} \quad (16)$$

$$[\eta] = \frac{\eta_{sp}/c}{1 + 0.45\eta_{sp}} \quad (17)$$

in water at 30 °C, where $[\eta]$, $[\eta]_{sp}$, and c are the intrinsic viscosity, specific viscosity, and polymer concentration in g/L, respectively. Table II shows the moments of degree of polymerization and the heterogeneity indexes $\langle n_i\rangle_w/\langle n_i\rangle_n$ and $\langle n_i\rangle_z/\langle n_i\rangle_w$ for i = d and h. They were obtained by a GPC measurement on the corresponding PVA derivatives, i.e., poly(vinyl N-phenylcarbamate)s.[21] Since the observed relationship between different average degrees of polymerization was different from the theoretically expected one, i.e., eq 15, we used the values obtained from GPC in the rest of this paper. The tacticity, degree of saponification, and degree of polymerization of d-

Table II
Moments of the Degree of Polymerization

	viscometry				GPC[a]	
code	$\langle n\rangle_v$	$\langle n\rangle_n$	$\langle n\rangle_w$	$\langle n\rangle_z$	$\langle n\rangle_w/\langle n\rangle_n$	$\langle n\rangle_z/\langle n\rangle_w$
d-PVA1850	1850	1270	3130	6030	2.47	1.934
h-PVA1750	1750	1525	2875	4851	1.88	1.69

[a] GPC measurement was conducted on the corresponding PVA derivatives, poly(vinyl *N*-phenylcarbamate).

PVA1850 are very close to those of h-PVA1750. Hence we expected no phase separation on mixing.

A 50/50 (by weight) mixture of d-PVA and h-PVA powder was dissolved in boiling distilled water. The solution of ca. 10 wt % was stirred for a few hours at 90 °C and then cooled gradually to room temperature. Films of the PVA mixture were prepared by solution casting onto a glass plate at 60 °C. The thickness of the films was around several hundred micrometers.

The films were coextruded with a poly(oxymethylene) billet at 165–170 °C at a crosshead speed of 1 mm/s. The extension draw ratio (EDR) was varied by changing the aspect ratio of the conical die. Coextrusion with an EDR larger than 5 was difficult because of the extruded film becoming inhomogeneous.

2. Small-Angle Neutron Scattering. Small-angle neutron scattering (SANS) experiments were conducted at the National Institute of Standards and Technology. A combination of cold neutrons of 9-Å wavelength and a focusing collimation system was employed to improve the spatial resolution. The incident beam was collimated by a series of holes with different diameters to converge the beam at the detector plane. The entrance and exit slit diameters are 9 and 4 mm, respectively, and they are 4.1 m apart. The exit slit to detector distance is 3.6 m. The sample to detector distance is 3.6 m. The incident beam profile on the detector is nearly triangular in shape, having FWHM = 1.3 mrad. The wavelength distribution is also approximated to be triangular, having FWHM = 2.25 Å. The details of the performance of the NIST facility were reported by Glinka et al.[17] The range of the magnitude of scattering vector covered was between 0.005 and 0.1 $Å^{-1}$. Scattered intensity was corrected for detector inhomogeneity, incoherent scattering, absorption, and so on. A circular average on a two-dimensional scattered intensity profile was taken for undeformed PVA, whereas a sector average of 10 deg was taken along directions both parallel and perpendicular to the extension direction for deformed samples.

3. Birefringence Measurement. A Cary-14 spectrophotometer operated in the visible range was used to determine the birefringence of the samples. The sample was placed between two high-extinction polarizers set at 90° relative to each other. The angle of the orientation direction of the sample was set at 45° to the axes of the polarizers. The spectral transmittance of this train of optical elements consists of a pattern of maxima and minima. The linear retardation, Γ, of the sample is related to the wavelength (λ) at which the extreme occurs by the following relations: maxima, $\Gamma_{max} = N\lambda_{max}$; minima, $\Gamma_{min} = (N + 1/2)\lambda_{min}$; N is an integer and denotes the order of extinction.

The birefringence (Δ_n) of a given specimen can therefore be deduced from the relation $\Gamma = \Delta_n t$, where t is the specimen thickness.

The number of maxima and minima was sufficiently large and the dependence of Γ on λ was such a weak one that the value of Γ at the wavelength of green light can be determined rather precisely.

Results and Discussion

1. Instrumental Smearing Effects. Before the discussion of the SANS results, we examine here the instrumental smearing effects for the evaluation of the radius of gyration. As discussed by Wignall et al.,[13] the smearing effects resulted from (1) the finite divergence of the beam, (2) the finite resolution of the detector, and (3) the polychromatic nature of the beam, and a Monte Carlo simulation technique was used to generate a smeared intensity curve from a model function. Lo[2] employed this technique and found that the nominal $I(0)$ value evaluated from a Zimm plot may have an error of more than 50% for a coextruded polystyrene film of EDR = ca. 10. This is the case for the experiments carried out at the 30-m SANS facility at Oak Ridge (ORNL), and only a very limited q range was used to evaluate radius of gyration because of the Guinier criterion. The standard deviation of the scattering vector q, σ_q, can be expressed in terms of the following equation[17]

$$\sigma^2_q = (k^2/4)[(R_1/L_1)^2 + (R_2/L')^2 + (2/3)(\Delta_D/L_2)^2 + (2/3)\theta^2(\Delta_\lambda/\lambda_N)^2] \quad (18)$$

where $k = 2\pi/\lambda_N$ (λ_N being the wavelength of a neutron) and R_1 and R_2 are the radii of the apertures of the entrance and exit slits. L_1 and L_2 are the distances between the entrance slit and exit slit and between the exit slit and the detector, respectively. L' is the effective length defined by $L_1L_2/(L_1 + L_2)$. Δ_D and Δ_λ are the FWHM of the detector resolution and the wavelength, respectively, σ_q's for NIST and ORNL facilities were estimated to be 7.68×10^{-4} Å and 14.5×10^{-4} Å at $q = 0$, respectively. The following parameters were used at the ORNL facility: $L_1 = 7.5$ m, $L_2 = 19$ m; $R_1 = 0.75$ cm, $R_2 = 0.5$ cm. The values of the wavelengths were chosen to be 9 and 4.75 Å respectively for NIST and Oak Ridge. Therefore there is no significant difference in angular resolution between these two facilities at $q = 0$. σ_q for the NIST facility, however, increases faster with q than that of ORNL because of the broad distribution of the wavelength.

Calculations were conducted to estimate the smearing effects at the NIST facility. Both random-coil (Debye function) and hard-sphere models were used to generate data between 0.005 and 0.020 $Å^{-1}$. The results indicted that for R_g less than 200 Å the smearing introduced an error less than 5% for both models. This point was verified experimentally; a calibration standard from ORNL with R_g of 207 Å was measured and a value of 199 Å was obtained.

With R_g greater than 200 Å the instrumental smearing is detrimental to the scattering data for the hard-sphere model; an error greater than 50% was observed for R_g = 350 Å. However, for the random-coil model the error caused by instrumental smearing remained less than 20% with R_g up to 700 Å, which is near the upper limit of our experimental results. Apparently, this estimated error depends strongly on the model chosen and the q range used. For this model calculation a range of 0.005–0.020 $Å^{-1}$ was used, in accordance with the experimental condition. As mentioned in the foregoing section, the SANS data were fitted with a Debye function to find R_g. For the magnitude of R_g encountered in this work, the error due to the smearing effect is about 20% if the choice of the random-coil model is a correct one. Otherwise the error could be significantly larger.

2. Radii of Gyration of Undeformed PVAs. Two sets of PVA isotope blends were analyzed in order to check the molecular weight dependence of the radius of gyration. One is a blend of d-PVA900 and h-PVA1750 and the other is d-PVA1850 and h-PVA1750. The scattered intensity was plotted in the form $I^{-1}(q)$ versus q^2 (Zimm plot) and a nonlinear least-square regression was conducted by using eq 10. Figure 1 shows the plot of $I^{-1}(q)$ versus q^2 for an undeformed PVA film of d-PVA1850/h-PVA1750. The circles and the curve denote the observed data points and the calculated intensity curve, respec-

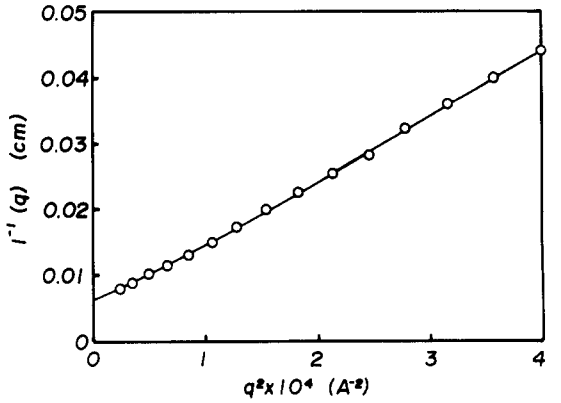

Figure 1. Plot of $I^{-1}(q)$ versus q^2 for an undeformed PVA film of d-PVA1850/h-PVA1750. The circles and solid line denote the observed data points and the calculated curve, respectively.

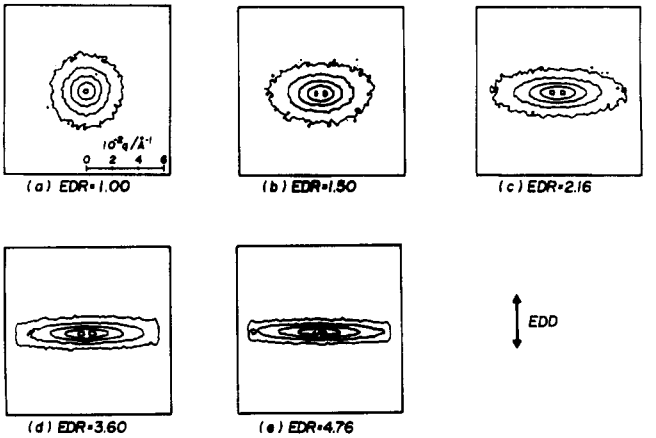

Figure 2. Scattered intensity contour curves for an undeformed PVA film (a) and for coextruded PVA films with an extension draw ratio (EDR) of 1.50 (b), 2.16 (c), 3.60 (d), and 4.76 (e). Each contour indicates an isointensity curve of 30, 60, 120, 240, and 480 cm^{-1}.

tively. The range of the curve fitting was between 0.005 and 0.02 Å^{-1}. The estimated radii of gyration of deutereous PVA were 183 and 143 Å, respectively, for d-PVA1850 and d-PVA900. The estimated radii of gyration should scale to the root square of the degrees of polymerization. The ratio of the estimated radii, however, is 1.27 whereas the square root of the ratio of the degrees of polymerization is 1.43. This discrepancy may result from the uncertainty of molecular weight determination. By taking into account the experimental error, the radius of gyration is estimated as

$$(R_{g,i})_0 = (b/6^{1/2})\langle n_i \rangle_z^{1/2} \approx 2.43\langle n_i \rangle_z^{1/2} \quad (19)$$

for i = d and h. The best fitted value for the segment length, b, is ca. 5.96 Å. This value is between the values appearing in the Polymer Handbook,[22] 6.3 Å, and in the paper by Matuo and Inagaki,[23] 4.09 Å, for a PVA–water system. This discrepancy may result mainly from the uncertainty of the molecular weight measurement.

3. Radii of Gyration of Coextruded PVAs. Figure 2 shows the scattered intensity contour curves for undeformed PVA film (a) and for coextruded PVA films at the extension draw ratios (EDR) of 1.50 (b), 2.16 (c), 3.60 (d), and 4.76 (e). Each contour indicates an isointensity curve of 30, 60, 120, 240, and 480 cm^{-1}. With increasing EDR, the patterns are flattened in the direction perpendicular to the extension draw direction, indicating that chains are deformed in the extension direction.

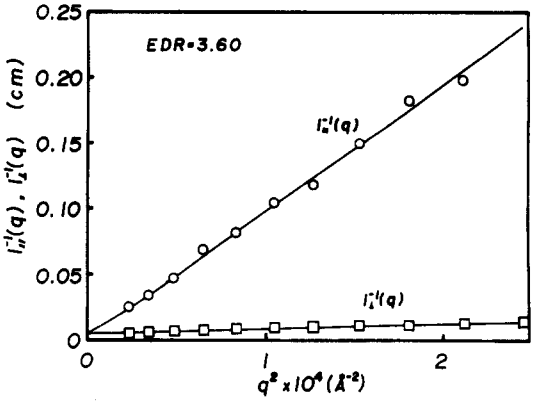

Figure 3. Inverse scattered intensities along the directions parallel and perpendicular to the extension direction, $I^{-1}{}_{\parallel}(q)$ and $I^{-1}{}_{\perp}(q)$, as a function of q^{-2} for the sample of EDR = 3.60. The open circles, open squares, and solid lines denote the observed data points for the parallel and perpendicular directions and the calculated curves, respectively.

Table III
Radii of Gyration of d-PVA

		Zimm[b]		deformed Gaussian chain		
					$R_{g\parallel}$	
EDR	MDR[a]	$R_{g\perp}$	$R_{g\parallel}$	$R_{g\perp}$[c]	direct[c]	contour
1.00	1.00	242	242	183	183	182
1.50	1.43	211	430	179	303	305
2.16	2.04	161	708	127	420	368
3.60	2.97	140		124	661	625
4.76	3.92	122		111	575	818

[a] Estimated from isointensity curves. [b] Estimated from a Zimm plot by using eq 13. [c] Estimated by using eq 10.

Figure 3 shows the inverse scattered intensities along the directions parallel and perpendicular to the extension direction, $I^{-1}{}_{\parallel}(q)$, $I^{-1}{}_{\perp}(q)$, as a function of q^{-2} for the sample EDR = 3.60. The open circles, open squares, and solid lines denote the observed data points for the parallel and perpendicular directions and the calculated curves, respectively. The range of the curve fitting was between 0.005 and 0.015 Å. The observed data points were well fitted by the calculated curves. In addition, both $I^{-1}{}_{\parallel}(q)$ and $I^{-1}{}_{\perp}(q)$ approach a point at $q = 0$, indicating that the molecular weight obtained from the scattered intensity at $q = 0$ is independent of the direction of observation. The R_g values along the directions parallel and perpendicular to the extension direction estimated from this figure were 660 and 124 Å, respectively. Similarly, the radii of gyration were evaluated for EDR = 1.50, 2.16, and 4.76. The evaluated radii of gyration were corrected for the wavelength distribution smearing effect. Table III summarizes the R_g values of d-PVA chains for undeformed and coextruded films. The extension draw ratio is given in column 1 and the molecular draw ratio estimated from the isointensity contour scheme (eq 14) is listed in column 2. The values of R_g in both the parallel and the perpendicular directions were estimated from a Zimm plot (eq 13), and the results are listed in columns 3 and 4. The values from the Zimm plot seem to be an overestimation because the q range used in linear regression was bigger than the Guinier limit of $qR_g < 1$. The estimated values from a nonlinear regression fit based on eq 10 are listed in columns 5 and 6 under the heading of deformed Gaussian. The best-fit value of $R_{g\parallel}$ for the case of EDR = 4.76 cannot be estimated reliably because the data points are scattered. Alternatively, the

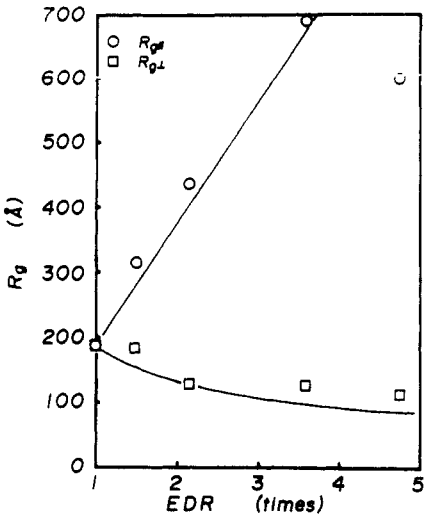

Figure 4. Variation of $R_{g\parallel}$ and $R_{g\perp}$ as a function of EDR. The open circles and squares show the calculated $R_{g\parallel}$ and $R_{g\perp}$ by the direct curve-fitting method. The solid lines show the values based on the assumption of affine deformation.

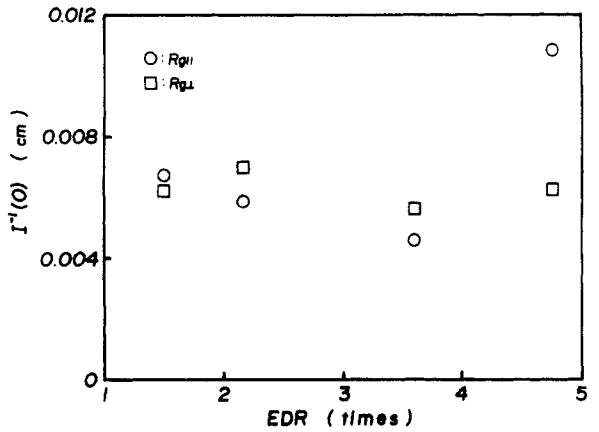

Figure 5. Inverse scattered intensity, $I^{-1}(0)$, as a function of EDR.

values of $R_{g\parallel}$ were calculated as the products of $R_{g\perp}$ of column 5 and MDR of column 2, and the results are given in column 7 as a reference.

Figure 4 shows the variation of $R_{g\parallel}$ and $R_{g\perp}$ as a function of EDR. The open circles and squares denote $R_{g\parallel}$ and $R_{g\perp}$ calculated from a nonlinear regression fit using eq 10. The solid lines denote the theoretical values based on the assumption of affine deformation. This shows that PVA chains are deformed affinely at least up to EDR = ca. 4. The deviation of $R_{g\parallel}$ for EDR = 4.76 from the affine assumption is discussed as follows.

Figure 5 shows the $I^{-1}(0)$ values in the perpendicular directions as a function of the extension draw. Since $I^{-1}(0)$ is related to the weight-average degree of polymerization, it should not change on deformation unless molecules are scissored. This plot is useful to check void formation on extension as well as the validity of the nonlinear regression analysis. If voids are formed on extension, $I(0)$ should increase so that $I^{-1}(0)$ decreases with EDR. Similarly, if the nonlinear regression does not work well, it will give an unreasonable $I^{-1}(0)$ value. Figure 5 shows that $I^{-1}{}_{\perp}(0)$ values are constant within an experimental error until EDR reaches 4.76. The $R_{g\parallel}$ value of EDR = 4.76 calculated by using the nonlinear regression reveals some anomaly; its value is smaller than that of EDR = 3.60.

The weight-average degree of polymerization estimated from $I(0)$ was 3720, which is close to the value

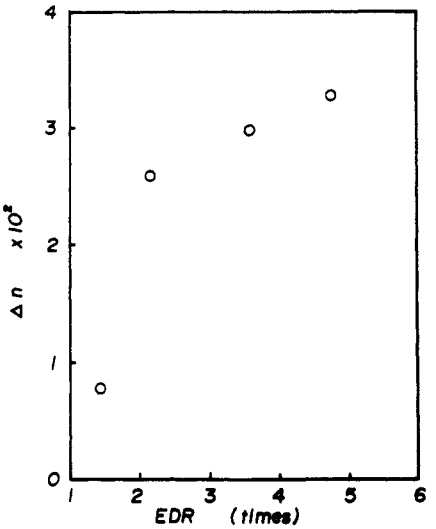

Figure 6. Birefringence of the deformed PVA films as a function of EDR.

measured by GPC, 3130. On the other hand, the weight-average degree of polymerization estimated from the value obtained from viscometry by assuming the most probable distribution of the molecular weights is 2030, which is much smaller than those observed by SANS and by GPC. This discrepancy in degree of polymerization may result mainly from the relationship between degree of polymerization and intrinsic viscosity, i.e., eqs 16 and 17. Although these equations have been used to characterize PVA, the exact relationship between the viscosity-average degrees of polymerization and the intrinsic viscosity has to be re-examined.

4. Birefringence and Orientation Factor. Figure 6 shows the birefringence of the deformed PVA films as a function of EDR. Since the intrinsic birefringence of PVA is 4.43×10^{-2},[24] the increase in birefringence with EDR is remarkably high. If the system is composed of two phases (crystal and amorphous), the birefringence is given by

$$\Delta = X_c f_c \Delta^\circ_c + (1 - X_c) f_a \Delta^\circ_a \tag{20}$$

where f_i and Δ°_i are the orientation factor and intrinsic birefringence of amorphous (a) and crystal (c) phases, respectively, and X_c is the degree of crystallinity. Form birefringence is neglected. In the case of PVA, since we know $f_a \approx f_c = f$ for large EDR,[18,26] i.e., EDR > 1, and Δ°_a is only slightly smaller than Δ°_c, we assume

$$\Delta \approx f \Delta^\circ_c \tag{21}$$

Figure 7 shows the estimated orientation factor from eq 21. The solid line in the figure shows the calculated orientation factor based on a floating rod model proposed by Kratky[27] and using the value of MDR as the macroscopic deformation ratio. The calculated orientation factor is given by

$$f = [3\langle \cos^2 \theta \rangle - 1]/2 \tag{22}$$

where

$$\langle \cos^2 \theta \rangle = [\alpha^3/(\alpha^3 - 1)]\left[1 - \frac{\tan^{-1}(\alpha^3 - 1)^{1/2}}{(\alpha^3 - 1)^{1/2}}\right] \tag{23}$$

where θ is the angle between molecular axis and the stretching direction and α is the molecular draw ratio MDR. As shown in the figure and listed in Table IV, the calculated values of birefringence are very close to the observed ones. It is noteworthy that the orientation factor increases

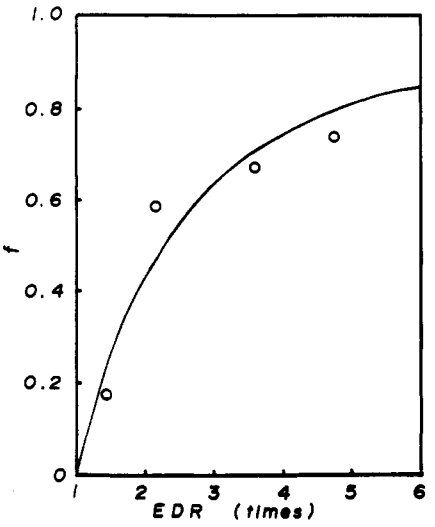

Figure 7. Estimated orientation factor from eq 21. The solid line in the figure shows the calculated orientation factor based on a floating rod model and by assuming that EDR is equal to MDR.

Table IV
Birefringence of PVA Films

EDR	$10^3\Delta$	Δ/Δ° [a]
1.50	1.71	0.176
2.16	2.59	0.585
3.60	2.97	0.671
4.76	3.28	0.740

[a] Δ°, the intrinsic birefrigence of PVA; $\Delta^\circ = 4.43 \times 10^{-2}$.

to 0.74 at EDR = 4.76. Nomura and Kawai also observed high values for orientation factors in isotactic and syndiotactic PVA as well as in atactic PVA.[26] This value is surprisingly larger than the value reported by Lo for polystyrene[2] where $f = 0.29$ for EDR = 9.5. In the case of polystyrene, affine deformation was observed until the value of EDR reached 9.5. This comparison illustrates that PVA chains are deformed more effectively by coextrusion than polystyrene. A possible explanation is that the hydrogen bonding in PVA films prevents slippage of chains on deformation and effectively transfers the external strain to the molecular level.

In the case of deformed polymer networks, the molecular draw ratio is much smaller than the expected value from affine deformation and networks behave like phantom chains.[28] In addition, swelling results in very little change in the radius of gyration. This behavior is explained by topological rearrangement of network chains. Candau et al.[29] discussed that affine deformation could be expected for highly cross-linked networks since topological rearrangement became less probable. This may be the case for the PVAs studied here since a high density of "cross-links" due to hydrogen bonding is quite likely. This phenomenon can be considered a positive effect of hydrogen bonding on extension.

Further investigation of crystal orientation is now being conducted using wide-angle X-ray diffraction, which will be reported in a forthcoming paper.[30]

Conclusion

Chain dimensions of undeformed PVA were measured by small-angle neutron scattering. The statistical segment length for PVA is found to be 5.96 Å. Chain asymmetry of solid-state coextruded PVA was examined by both small-angle neutron scattering and birefringence measurements. It was found that PVA chains were affinely deformed for extension up to EDR = ca. 5. Birefringence measurements also show the affine nature of the deformation of PVA chains. Birefringence measurements show that PVA is more effectively deformed than polystyrene, which is explained by a positive effect of hydrogen bonding on extension.

Acknowledgment. We are greatly indebted to Kuraray Co., Ltd., for their kindness in providing deutereous poly(vinyl alcohol). Thanks are also due to Prof. T. Kanamoto, Tokyo Science University, for collaboration, many suggestions, and helpful discussions. This work was supported in part by a grant-in-aid, Monbusho International Research Program, Joint Research (No. 63044083) and by a contract with the Office of Naval Research. We are also indebted to the reviewer for suggestions regarding the incidental smearing effects and for improvement of the paper.

References and Notes

(1) Hadziioannou, G.; Wang, L.; Stein, R. S.; Porter, R. S. *Macromolecules*, **1982**, *15*, 880.
(2) Lo, R. Ph.D. Dissertation, University of Massachusetts, 1986.
(3) Tuboi, K.; Mochizuki, T. *Kobunshi Kagaku* **1966**, *23*, 636; **1967**, *24*, 433.
(4) For example: Sakurada, I. *Polyvinyl Alcohol Fibers*; Marcel Dekker; New York, 1985.
(5) Benoit, H.; Duplessix, R.; Ober, R.; Daoud, M.; Cotton, J. P.; Farnoux, B.; Jannink, G. *Macromolecules* **1975**, *8*, 451.
(6) Pearson, D. J. *Macromolecules* **1977**, *10*, 696.
(7) Warner, M.; Edwards, S. F. *J. Phys. A: Math. Gen.* **1978**, *11*, 1649.
(8) Nierlich, M.; Williams, C.; Boue, F.; Cotton, J. P.; Daoud, M.; Farnoux, B.; Jannink, G. *J. Appl. Crystallogr.* **1978**, *11*, 504.
(9) de Gennes, P.-G. *Scaling Concepts in Polymer Physics*; Cornell University Press: Ithaca, NY, 1979; Chapter 4.
(10) This assumption was made for the following reasons: The Flory interaction parameter is very small for isotope mixture[10a] and it does not affect the evaluation of R_g. (a) See for example: Bates, F. S.; Wignall, G. D. *Phys. Rev. Lett.* **1986**, *57*, 1429.
(11) Ullman, R. *J. Polym. Sci., Polym. Lett. Ed.* **1983**, *22*, 521.
(12) Ullman, R. *J. Polym. Sci., Polym. Phys. Ed.* **1985**, *23*, 1477.
(13) Wignall, G. D.; Christen, D. K.; Ramakrishnan, V. *J. Appl. Crystallogr.* **1987**, *20*, 28.
(14) Tanzer, J. D.; Crist, B. *J. Polym. Sci.* **1989**, *B27*, 859.
(15) Tanzer, J. D.; Bartels, C. R.; Crist, B.; Graessley, W. W. *Macromolecules* **1984**, *17*, 2708.
(16) Shibayama, M.; Yang, H.; Stein, R. S.; Han, C. C. *Macromolecules* **1985**, *18*, 2179.
(17) Glinka, C. J.; Rowe, J. M.; LaRock, J. D. *J. Appl. Crystallogr.* **1986**, *19*, 427.
(18) Bamford, C. H., Barb, W. G., Jenkins, A. D., Onyon, P. R. *Kinetics of Vinyl Polymerization by Radical Mechanism*; Butterworth: London, 1958; Chapter 7.
(19) Ueda, M.; Nakao, Y.; Kajitani, K. Unpublished results.
(20) Japan Industry Standard, JIS-K 6726.
(21) Kajitani, K., Kuraray Co., Ltd., Private Communication.
(22) Brandrup, J., Immergut, E. H., Eds. *Polymer Handbook*; Wiley: New York, 1975; Chapter IV-4.
(23) Matuo, T.; Inagaki, H. *Makromol. Chem.* **1963**, *54*, 150.
(24) *Sen-i Binran, Raw Material*; Gakkai, S.-i., Ed.; Maruzen: Tokyo, 1968.
(25) Unpublished data.
(26) Nomura, S.; Kawai, H. *J. Polym. Sci., Part A-2* **1966**, *4*, 797.
(27) Kratky, O. *Kolloid-Z.* **1933**, *64*, 213.
(28) Beltzung, M.; et al. *Proc. 27th International Symposium on Macromolecules*; Strasburg, 1981; p 728.
(29) Candau, S.; Bastide, J.; Delsanti, M. *Adv. Polym. Sci.* **1982**, *44*, 30.
(30) Shibayama, M.; Nomura, S. Manuscript in preparation.

Registry No. PVA, 9002-89-5.